Official Dental Journal of Suez Canal University
DENTAL SCIENCE Updates
Print ISSN 2636-3836
Online ISSN 2636-3844
www.dsujournals.ekb.eg
DSU — Vol. 6, No. 2, September (2025) — PP. 429:439

IN-VITRO INVESTIGATION OF THE MICROSTRUCTURE, ELEMENTAL ANALYSIS AND MICROHARDNESS OF THREE HYBRID RESIN MATERIALS USED AS SINGLE-TOOTH RESTORATIONS

Noha Saadoun[1], Mohamed Sherif Mohamed Salah Eldin Farag[2], Rania El-Saady Badawy[3]

DOI: 10.21608/dsu.2025.385544.1303
Manuscript ID: DSU-2505-1303

KEYWORDS

CAD/CAM materials, Microhardness, Microstructure, Three-dimensional printing.

• E-mail address: Noha.Saadoun@den.suezuni.edu.eg

1. Assistant Lecturer of Dental Biomaterials, Faculty of Dentistry, Suez University, P.O.Box: 43221, Suez, Egypt.
2. Professor of Pediatric, Preventive Dentistry and Dental Public Health, Faculty of Dentistry, Suez Canal University, Ismailia, Egypt.
3. Professor of Dental Biomaterials, Faculty of Dentistry, Suez Canal University, Ismailia, Egypt.

ABSTRACT

Introduction: Technology constantly evolves, leading to the extensive usage of CAD/CAM techniques (subtractive and additive manufacturing) to produce indirect restorations. Nowadays, hybrid resin materials are commonly used to fabricate single-tooth permanent restorations. **Aim of the study:** The current study evaluated and compared three commercially available hybrid resin materials used for additive and subtractive manufacturing of single-tooth permanent restorations. **Methodology:** 75 bar-shaped specimens (14 x 2 x 2 mm) of 3 different hybrid resin materials were used in this study and classified into 3 main groups. Lava Ultimate group (n=15), Vita Enamic group (n=15), and Flexcera Smile Ultra$^+$ group (n=45). Flexcera Smile Ultra$^+$ group was further subdivided into 3 subgroups (n=15): Flexcera Smile Ultra$^+$ A (0-degree printing angle), Flexcera Smile Ultra$^+$ B (45-degree printing angle), and Flexcera Smile Ultra$^+$ C (90-degree printing angle). Specimens were investigated regarding microstructure, elemental analysis, and surface microhardness. One-way ANOVA and Kruskal-Wallis tests were used for statistical data analysis. **Results:** Scanning electron microscopic images showed typical hybrid resin materials with irregularly shaped fillers and different sizes embedded in the resin matrix. Flexcera Smile Ultra$^+$ specimens showed the highest statistically significant carbon median value (42.65 wt.%). Lava Ultimate specimens showed the highest statistically significant silicon and zirconium median values (27.15 and 16.38 wt.%, respectively). Vita Enamic specimens showed the highest statistically significant aluminum median value (9.15 wt.%) and surface microhardness mean value (205.02). **Conclusions:** The 3D printed material had higher resin content, lower filler content, and lower surface microhardness than CAD/CAM blocks. Specimens printed with a 45-degree angle showed the best microhardness results.

INTRODUCTION

To restore the function and aesthetics of teeth that have suffered severe hard tissue loss as a result of caries, root canal therapy, wear, or coronal fractures, indirect restorations are required [1,2]. Nowadays, CAD/CAM systems are frequently utilized in labs and clinics to fabricate indirect, superior restorations with less time and effort [1-3]. Subtractive manufacturing of blocks and discs enabled the production of reliable restorations with accurate dimensions in a short manufacturing time [4,5].

Combining the benefits of resin composites and ceramics is the aim of creating resin matrix nanoceramic materials and polymer-infiltrated ceramic networks as substitutes for glass ceramics[1,3,6]. These materials

have many benefits, such as easy fabrication, mechanical properties close to those of natural teeth, and the possibility of intraoral repair [1,7].

A drawback of the subtractive technique is that the millable shape is limited by the size of the cutting bur and the range of motion of the cutting device[5,8]. This leads to the loss of blocks' unused parts, waste of raw materials, and more difficult recycling of excess material. Furthermore, the milling process may result in considerable wear of the cutting tools and microscopic cracks, which could weaken the restorations [9].

Lately, dentistry has seen a significant expansion in additive manufacturing (AM) applications, also known as 3D printing. In AM, material is deposited in layers to form 3D objects [10,11]. Even though AM has many advantages, such as easy production of objects with complex structures, material savings, and lower cost than the milling process [5,12], it still has some disadvantages. The main drawbacks of AM are low filler content and mechanical anisotropy as a result of the layered fabrication technique used[13,14].

The most promising AM techniques for creating accurate designs with fine surface finishing are stereolithography (SLA) and digital light processing (DLP) [15]. The printing orientation also significantly impacts the material's characteristics, product accuracy, and biocompatibility. Other factors that can affect the final printing outcomes include layer thickness and post-curing [16,17].

Nowadays, hybrid resin materials (resin matrix ceramics) have been a practical option for 3D printed single tooth restorations. Even though these materials' mechanical and physical characteristics have been studied, their performance remains controversial [1,3,18,19]. More research is needed to assess these materials' long-term behavior before they can be widely recommended for various types of permanent restorations for a single tooth[1]. Therefore, it was interesting to investigate the structure and surface hardness characteristics of three commercially available hybrid resin materials recommended for permanent single-unit restorations. The null hypothesis was that there would be no significant differences in microstructure, elemental analysis, and microhardness between hybrid resin materials for milling and printing.

MATERIALS AND METHODS

Approval of the Ethics Committee of Scientific Research, Faculty of Dentistry, Suez Canal University, had been obtained before starting the study with approval number (584/2022).

1. Specimens' preparation and grouping

Seventy-five bar-shaped specimens of the three different hybrid resin materials were used in this study. The specimens were classified into three main groups: The Lava Ultimate group (LU grp, n=15), the Vita Enamic group (VE grp, n=15), and the Flexcera Smile Ultra$^+$ group (FSU$^+$ grp, n=45). The FSU$^+$ group was subdivided into three subgroups (n=15): the FSU$^+$ A, the FSU$^+$ B, and the FSU$^+$ C.

Lava Ultimate and Vita Enamic blocks were cut with a low-speed water-cooled diamond microsaw (Isomet 4000, Buehler, Germany) (Fig.1a) to obtain bar-shaped specimens, 14 mm length, 2 mm width and 2 mm thickness (Fig. 1b and 1c) ensuring their dimensions using a digital caliper (TMT321506 IP54, Micro Ohm Electronics, Cairo, Egypt) (Fig. 1d). After that, specimens were finished with 220 grit wet silicon carbide (3M ESPE, Saint Paul, MN, USA) and then kept dry at room temperature [2]. Because of the size of the material blocks, it was not possible to prepare the specimens in accordance with ISO 4049 [20].

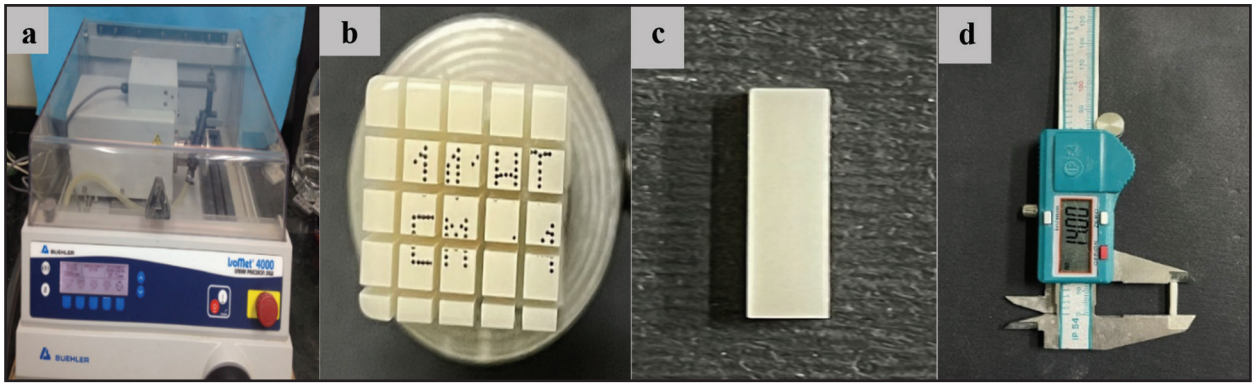

Fig. (1) **(a)** Low-speed water-cooled diamond microsaw used in the study (Isomet 4000, Buehler, Germany), **(b)** CAD/CAM block after cutting, **(c)** Bar-shaped specimen (14x2x2 mm), **(d)** Digital caliper used in the study.

A DLP 3D printer (Mogassam, Cairo, Egypt) (Fig.2a) was used to print the bar-shaped specimens of the three FSU+ subgroups (14 x 2 x 2mm) using Chitubox V1.9.1 software. FSU+ A subgroup specimens were printed with an angle of 0-degree (in a horizontal direction, parallel to the platform) (Fig.2b), while FSU+ B subgroup specimens were printed with an angle of 45-degree to the platform (Fig.2c), and FSU+ C subgroup specimens were printed with an angle of 90-degree (in a vertical direction, perpendicular to the platform) (Fig. 2d).

For FSU+ hybrid resin material, the resin profile has been optimized to have 5 mm for the lift distance, 60 mm/s for the lift speed, 0.05 mm for the layer height, 8 for the bottom layer count, 6.5 for the exposure time, and 20 for the bottom exposure [2, 21].

Following the manufacturer's recommendations, the printed specimens were cleaned with 99% ethyl alcohol and then subjected to a light-curing unit (Mogassam, Cairo, Egypt) (Fig. 3) twice for 45 minutes each, rotating after the first exposure. After the specimens were finished using the wet silicon carbide, the proper dimensions were confirmed using the digital caliper once more [2].

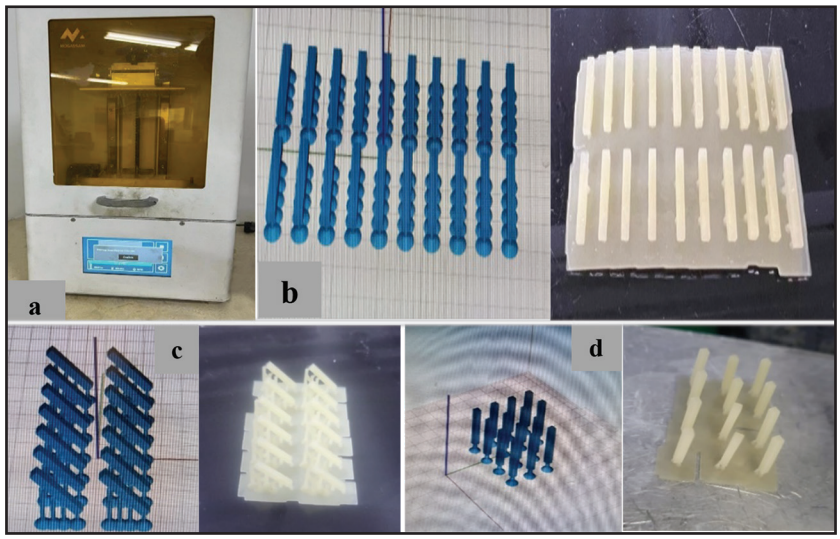

Fig. (2) **(a)** DLP 3D printer used in the study (Mogassam, Cairo, Egypt), **(b)** Bar-shaped specimens printed with an angle of 0-degree, **(c)** Bar-shaped specimens printed with an angle of 45-degree, **(d)** Bar-shaped specimens printed with an angle of 90-degree.

Fig. (3) Light-curing unit used in the study (Mogassam, Cairo, Egypt).

2. Microstructure and Elemental analysis testing

A total of 15 randomly selected bar-shaped specimens (n=5/grp) were examined without application of a coating layer to their surfaces. A scanning electron microscope (SEM) (Quanta 3D 200i, FEI Company, Netherlands) (Fig.4a) was used to examine the microstructure of the specimens (magnifications 250x up to 5000x). During the SEM investigation, large field electron (LFE) and back-scattered electron (BSE) detectors operating at a working distance of 15–17 mm were employed with an accelerating voltage of 20 kV under low vacuum. An energy dispersive X-ray spectroscopy (EDX) unit (Thermofisher Pathfinder) attached to the SEM was used to examine the elemental composition of the specimens.

3. Surface microhardness measurement

Seventy-five bar-shaped specimens (n=15/LU grp, VE grp, and each FSU$^+$ subgroup) were tested including the same specimens that were used before for microstructure and elemental analysis testing. Vickers microhardness test indenter (Wilson Tukon 1102, Buehler, Germany) (Fig. 4b) was used [100gf load (980.7mN) (HV0.1) and a 10s dwell time], making three indentations at random locations for each specimen. The Vickers hardness (HV) was calculated using the following equation: $HV = 1854.4L/d^2$, where the load L is in gf and the average diagonal d is in μm.

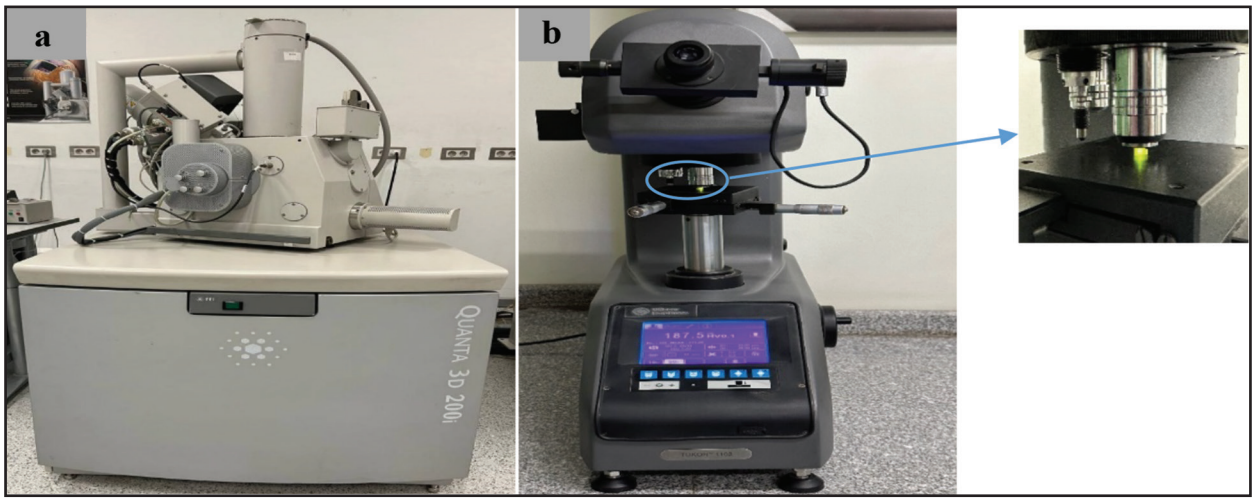

Fig. (4) **(a)** Scanning electron microscope (SEM) (Quanta 3D 200i, FEI Company, Netherlands) with Energy dispersive X-ray spectroscopy (EDX) unit (Thermofisher Pathfinder) attached to it (SEM-EDX) used in the study, **(b)** Vickers microhardness test indenter (Wilson Tukon 1102, Buehler, Germany) used in the study.

4. Statistical analysis and data interpretation

Data analysis was performed by SPSS software versions 26 (SPSS Inc., PASW statistics for windows version 26. Chicago: SPSS Inc.). Qualitative data were described using numbers and percentages, while quantitative data were described using mean ± standard deviation for normally distributed data and median (minimum and maximum) for non-normally distributed data after normality testing using Shapiro Wilk test. The results' significance was judged at the $p \leq 0.05$ level. The One-Way ANOVA test was used to compare more than two independent groups for normally distributed data, with the Post hoc Tukey test for pairwise comparisons. The Kruskal-Wallis test was used to compare more than two studied groups for non-normally distributed data, with the Mann-Whitney test for pairwise comparisons.

RESULTS

Microstructure and Elemental analysis

1. Microstructure examination (SEM examination)

Scanning electron microscopic assessment of the finished surfaces of the three different materials specimens showed the presence of fillers with varying particle diameters and contents. By inspection, LU specimens showed the highest filler content with homogeneous distribution, while FSU^{+} specimens showed the lowest. The size of the filler particles varied between around 340 nm for FSU^{+} and 11μm for VE. All specimens revealed an irregular shape of the filler particles, with bridging between filler particles only detected for VE specimens (Fig.5, 6 and 7).

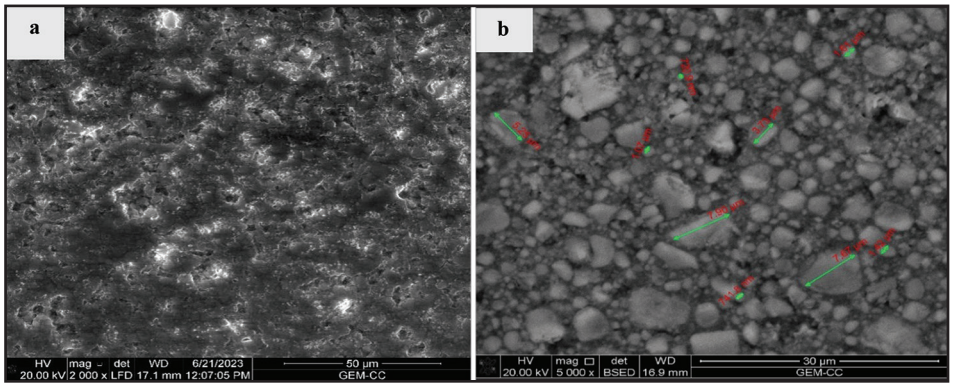

Fig. (5) SEM images of LU specimens. **(a)** SEM image showing hybrid content of resin and fillers (Magnification: 2000x, LFE detector), **(b)** SEM image showing filler size ranging from 720 nm to 8 μm (Magnification: 5000x, BSE detector).

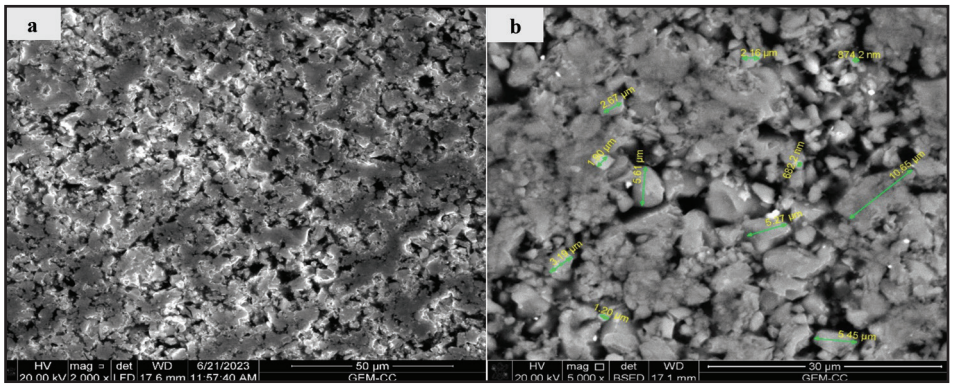

Fig. (6) SEM images of VE specimens. **(a)** SEM image showing hybrid content of resin and fillers with bridging between filler particles (Magnification: 2000x, LFE detector), **(b)** SEM image showing filler size ranging from 682nm to 11 µm (Magnification: 5000x, BSE detector).

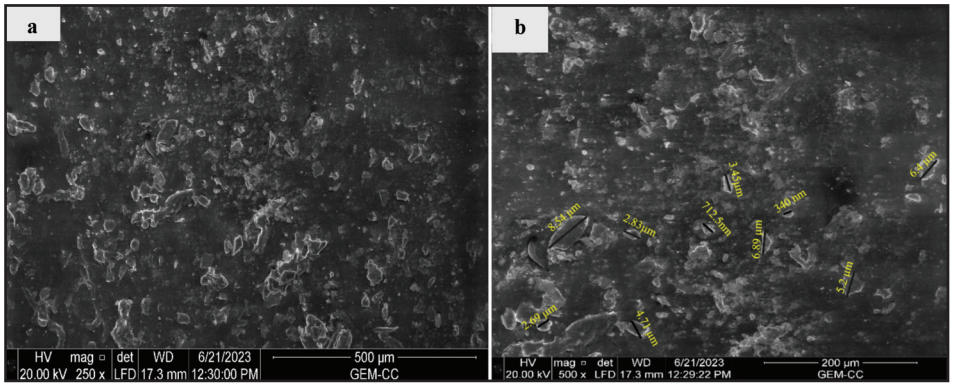

Fig. (7) SEM images of FSU+ specimens. **(a)** SEM image showing hybrid content of resin and fillers (Magnification: 250x, LFE detector), **(b)** SEM image showing filler size ranging from 340 nm to 8.54 µm (Magnification: 500x, LFE detector).

2. Elemental analysis (EDX A)

The EDX A results of the three different materials' specimens are represented in (Fig. 8). FSU+ specimens showed the highest carbon (C) median value (42.65 wt.%), while LU specimens showed the lowest C median value (13.02 wt.%). There was a statistically significant difference ($p \leq 0.05$) in C wt.% between FSU+ and LU groups on the one hand, and FSU+ and VE groups on the other hand.

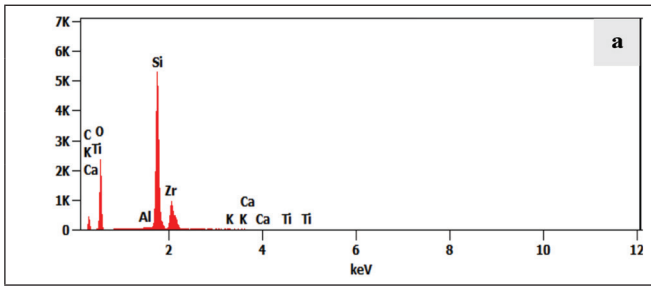

Element	Weight%
C	11.79
Si	27.4
Zr	16.77
Al	0.06

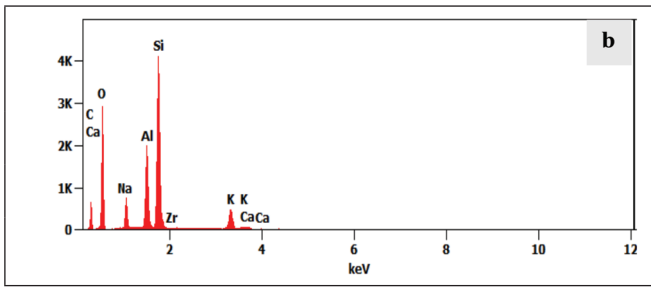

Element	Weight%
C	13.67
Si	23.21
Zr	0.17
Al	9.41

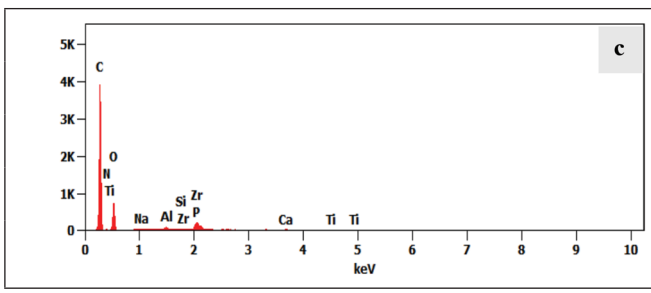

Element	Weight%
C	40.92
Si	0.17
Zr	4.42
Al	0.5

Fig. (8) Elemental analysis of three different materials' specimens. **(a)** EDX A. of LU specimen, **(b)** EDX A. of VE specimen, **(c)** EDX A. of FSU+ specimen.

Lava Ultimate specimens showed the highest silicon (Si) median value (27.15 wt.%), while FSU+ specimens showed the lowest Si median value (0.08wt.%). A statistically significant difference (p≤0.05) in Si wt.% among the tested groups.

Lava Ultimate specimens showed the highest zirconium (Zr) median value (16.38 wt.%), while FSU+ specimens showed the lowest Zr median value (0.14 wt.%). There was a statistically significant difference (p≤0.05) in Zr wt.% between LU and VE groups on the one hand, and LU and FSU+ groups on the other hand.

Vita Enamic specimens showed the highest aluminum (Al) median value (9.15 wt.%), while FSU+ specimens showed the lowest Al median value (0.11 wt.%). There was a statistically significant difference (p ≤0.05) in Al wt.% between VE and LU groups on one hand, and VE and FSU+ groups on the other hand. Median wt.% values (minimum and maximum) of the four elements (C, Si, Zr and Al) for the tested groups are represented in (Table 1 and Fig.9).

3. Surface microhardness

The surface microhardness values can be ordered from higher to lower as VE > LU > FSU+ B > FSU+ C > FSU+ A. VE group showed the highest surface microhardness mean value (205.02±8.13). On the other hand, FSU+ A subgroup showed the lowest surface microhardness mean value (20.64±0.56). There was a statistically significant difference (p≤0.05) among the tested groups, except between FSU+ A and FSU+ C subgroups. Mean and standard deviation (SD) values of surface microhardness (gf/μm^2) for the tested groups are represented in (Table 2 and Fig. 10).

Table (1) *Median wt.% values (minimum and maximum) of the four elements (C, Si, Zr and Al) for the tested groups.*

Element	LU	VE	FSU+	Significance	Within group significance
	Median (min-max)	Median (min-max)	Median (min-max)		
Carbon	13.02 (11.79-13.84)	15.36 (14.27-15.71)	42.65 (40.53-59.22)	KW=12.37 p 0.002*	p1=0.456 p2=0.0001* p3=0.001*
Silicon	27.15 (23.21-27.47)	22.92 (22.37-23.21)	0.08 (0.07-0.17)	KW=12.17 p=0.002*	p1=0.001* p2=0.001* p3=0.001*
Zirconium	16.38 (0.17-16.77)	0.205 (0.16-0.25)	0.14 (0.02-4.42)	KW=7.18 p=0.028*	p1=0.001* p2=0.001* p3=0.784
Aluminum	0.18 (0.06-9.41)	9.15 (9.15-8.96)	0.11 (0.07-0.66)	KW=5.56 p=0.062	p1=0.001* p2=0.362 p3<0.001*

*KW: Kruskal Wallis test, p1: difference between LU and VE, p2: difference between LU and FSU+, p3: difference between VE and FSU+, *statistically significant.*

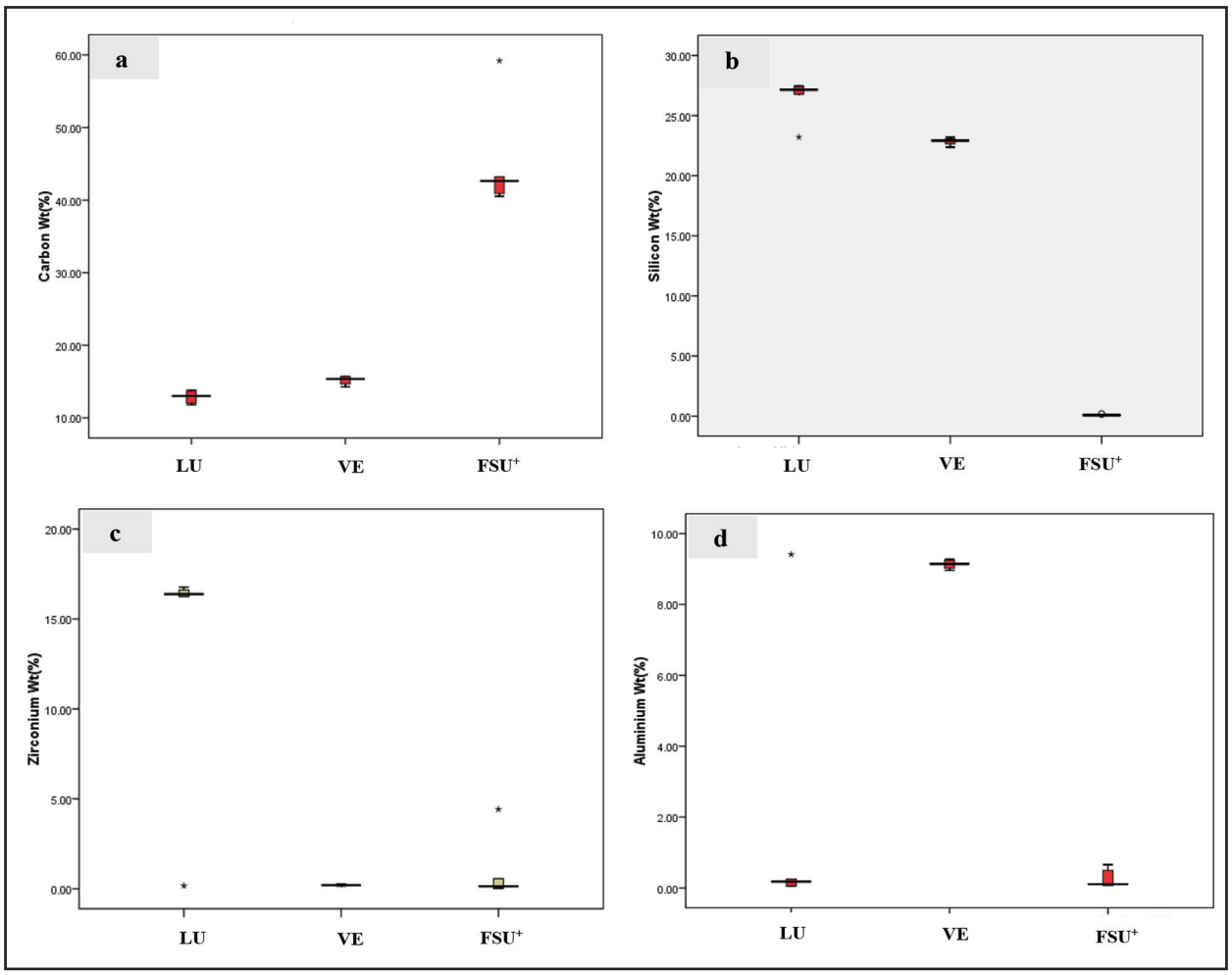

Fig. (9) Median wt.% values (minimum and maximum) of the four elements (C, Si, Zr and Al) for the tested groups [a, b, C and d].

Table (2) *Mean and standard deviation (SD) values of surface microhardness (gf/μm2) for the tested groups.*

Surface microhardness	LU	VE	FSU+ A (0 degree)	FSU+ B (45 degree)	FSU+ C (90 degree)	Test of significance
Mean ± SD	118.52±1.40[a]	205.02±8.13[b]	20.64±0.56[c]	27.96±5.13[d]	21.2±0.83[c]	F=1752.69 p <0.001*

*F: One-way ANOVA test, * statistically significant.*

Similar superscripted letters denote insignificant difference between studied groups within the same row by the Post Hoc Tukey test.

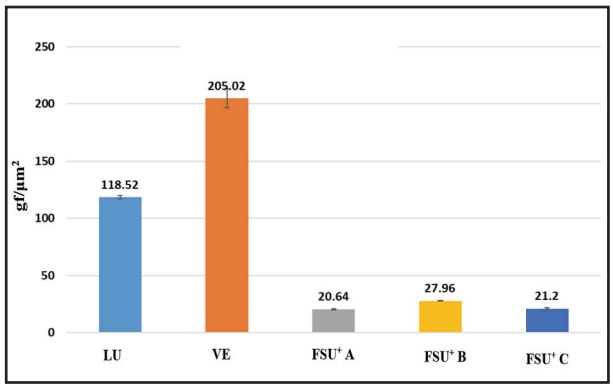

Fig. (10) Mean and standard deviation (SD) values of surface microhardness (gf/µm2) for the tested groups.

DISCUSSION

Additive manufacturing has drawn a lot of attention due to its expanded use in digital dentistry. 3D printing technology can be used to fabricate various restorations such as dental crowns and bridges. The two main 3D printing technologies used in dentistry are SLA and DLP. DLP has the advantage of faster printed layer production when compared to SLA. This allows a single layer to be printed and cured throughout the entire build platform in a matter of seconds. DLP also has the advantage of using less material than SLA and other 3D printing techniques, which lowers production costs[22]. The printing process is affected by 50 variables, with most manufacturers specifying them[23]. However, there are few recommendations for printing angle and orientation in software, making it crucial to evaluate restoration performance [21].

CAD/CAM's subtractive milling method offers numerous benefits, including digital scans, single-visit final restorations, and accurate, rapid prosthesis, eliminating traditional impressions, diagnostic casts, and temporary crown fabrication steps [24,25].

Polymer-based and hybrid resin materials are commonly used to fabricate dental crowns using CAD/CAM technologies [22]. Few studies have been conducted to assess the behavior of FSU⁺, a commercially available 3D-printed hybrid resin material. VE and LU are commonly used millable hybrid resin blocks. Further studies are still needed to evaluate their properties comparing them with 3D printed hybrid resin materials.

SEM-EDX analysis was used to determine the size and shape of fillers, as well as chemical composition of the three tested materials, as it is a reliable method commonly used for microstructure and elemental examination [2,26]. Our results showed that all tested materials had a structure that was typical for hybrid resin materials, with irregularly shaped fillers and of different sizes incorporated in the resin matrix. The LU specimens showed a homogeneous distribution of the filler particles; however, for VE, bridging between the filler particles and larger filler particle size were evident, being in accordance with previous studies [2,27].

According to EDX A results, the LU specimens mainly consist of silica and zirconia fillers with only a small amount of resin content (carbon content). This finding is in accordance with the manufacturer's product profile and previous studies [2,27,28]. The VE and LU specimens showed nearly equal resin contents (carbon contents), both showing a high silica fillers' content. The LU specimens were rich in zirconia fillers, while the VE specimens were rich in alumina fillers, being in accordance with previous studies [29,30]. The FSU⁺ specimens showed a high resin content (carbon content) and a low filler content, fulfilling the main requirement of flowability for printable materials [2].

A Vickers microhardness test (HV01) was used for assessment of the surface hardness of the tested groups, measuring the relative surface resistance

of the material to a square-based diamond pyramid indenter. Compared to other hardness tests, the Vickers hardness test is easier to use because it just requires calculations that are independent of the indenter's size, possibly used with different materials [31].

The VE group showed the highest microhardness values, being significantly different from other groups. This result is consistent with earlier studies showing that VE's structure, which includes a ceramic network, contributes to its high surface hardness [2,32]. Our results also revealed significantly higher microhardness values for the FSU+ B subgroup (printed with an angle of 45 degree) than those of the FSU+ A and FSU+ C subgroups. This may be due to its higher degree of conversion, which improves surface mechanical properties, being in accordance with an earlier study [2]. The null hypothesis was rejected based on the findings of this study.

Despite being a valuable study, it still has some limitations, including specimen dimensions and the Einstein 3D printer's recommendation by Desktop Health for FSU+ material, which may affect results accuracy. Further studies are needed to evaluate the effect of using different printers (including the Einstein 3D printer) on the properties of 3D printed hybrid resin materials, in addition to evaluating other properties such as fracture toughness, wear resistance, color stability, and biological properties.

CONCLUSIONS

Within the limitations of this study, the following can be concluded:

1. The 3D-printed hybrid resin material (FSU+) had higher resin content and lower filler content than millable CAD/CAM hybrid resin blocks (LU and VE).
2. The different printing angles (orientations) affected the surface microhardness of the 3D-printed FSU+ material, which was lower than that of LU and VE blocks.
3. Specimens printed at a 45-degree angle showed the best microhardness results compared to those printed at 0- and 90-degree angles.

REFERENCES

1. Mahran GA, El-Banna A, El-Korashy DI. Evaluation of a 3D-printed nanohybrid resin composite versus a milled resin composite for flexural strength, wear and color stability. BMC Oral Health 2025;25(1):572.
2. Grzebieluch W, Kowalewski P, Grygier D, Rutkowska-Gorczyca M, Kozakiewicz M, Jurczyszyn K. Printable and machinable dental restorative composites for CAD/CAM application-comparison of mechanical properties, fractographic, texture and fractal dimension analysis. MDPI 2021;14(17):4919.
3. Skorulska A, Piszko P, Rybak Z, Szymonowicz M, Dobrzyński M. Review on polymer, ceramic and composite materials for CAD/CAM indirect restorations in dentistry–application, mechanical characteristics and comparison. Mater (Basel) 2021;14(7):1592.
4. Bindl A, Mörmann WH. Marginal and internal fit of all-ceramic CAD/CAM crown-copings on chamfer preparations. J Oral Rehabil 2005;32(6):441-447.
5. Van Noort R. The future of dental devices is digital. Dent. Mater. J. 2012;28(1):3-12.
6. Çakmak G, Donmez MB, de Paula MS, Akay C, Fonseca M, Kahveci Ç, Abou-Ayash S, Yilmaz B. Surface roughness, optical properties, and microhardness of additively and subtractively manufactured CAD-CAM materials after brushing and coffee thermal cycling. J Prosthodont 2025;34(1):68-77.
7. Taşın S, Ismatullaev A. Effect of coffee thermocycling on the color and translucency of milled and 3D printed definitive restoration materials. J Prosthet Dent 2024;131(5):969-970.
8. Koch GK, Gallucci GO, Lee SJ. Accuracy in the digital workflow: From data acquisition to the digitally milled cast. J Prosthet Dent. 2016;115(6):749-754.

9. Wang H, Aboushelib MN, Feilzer AJ. Strength influencing variables on CAD/CAM zirconia frameworks. Dent Mater J 2008;24(5):633-638.
10. Dawood A, Marti BM, Sauret-Jackson V, Darwood A. 3D printing in dentistry. Br Dent J 2015;219(11):521-529.
11. Naseer MU, Kallaste A, Asad B, Vaimann T, Rassõlkin A. A review on additive manufacturing possibilities for electrical machines. MDPI 2021;14(7):1940.
12. Sun J, Zhang FQ. The application of rapid prototyping in prosthodontics. J Prosthodont 2012;21(8):641-644.
13. Unkovskiy A, Bui PH, Schille C, Geis-Gerstorfer J, Huettig F, Spintzyk S. Objects build orientation, positioning, and curing influence dimensional accuracy and flexural properties of stereolithographically printed resin. Dent Mater J 2018;34(12):324-333.
14. Alharbi N, van de Veen AJ, Wismeijer D, Osman RB. Build angle and its influence on the flexure strength of stereolithography printed hybrid resin material. An in vitro study and a fractographic analysis. Mater Technol 2019;34(1):12-27.
15. Komissarenko DA, Sokolov PS, Evstigneeva AD, Slyusar IV, Nartov AS, Volkov PA, et al. DLP 3D printing of scandia-stabilized zirconia ceramics. J Eur Ceram Soc 2021;41(1):684-90.
16. Park GS, Kim SK, Heo SJ, Koak JY, Seo DG. Effects of printing parameters on the fit of implant-supported 3D printing resin prosthetics. MDPI 2019;12(16):2533.
17. Jindal P, Juneja M, Bajaj D, Siena FL, Breedon P. Effects of post-curing conditions on mechanical properties of 3D printed clear dental aligners. Rapid Prototyp J 2020;26(8):1337-1344.
18. Pot GJ, Van Overschelde PA, Keulemans F, Kleverlaan CJ, Tribst JP. Mechanical properties of additive-manufactured composite-based resins for permanent indirect restorations: a scoping review. MDPI 2024;17(16):3951.
19. Ellakany P, Fouda SM, Mahrous AA, AlGhamdi MA, Aly NM. Influence of CAD/CAM milling and 3D-printing fabrication methods on the mechanical properties of 3-unit interim fixed dental prosthesis after thermo-mechanical aging process. Polym. J 2022;14(19):4103.
20. ISO 4049: Dentistry — Polymer-based restorative materials [Internet]; 2019. Available from: https://www.iso.org/standard/67596.html.
21. Keβler A, Hickel R, Ilie N. In vitro investigation of the influence of printing direction on the flexural strength, flexural modulus, and fractographic analysis of 3D-printed temporary materials. Dent Mater J 2021;40(3):641-649.
22. Alshamrani AA, Raju R, Ellakwa A. Effect of Printing Layer Thickness and Postprinting Conditions on the Flexural Strength and Hardness of a 3D-Printed Resin. Biomed Res Int 2022;2022(1):8353137.
23. Schaub DA, Chu KR, Montgomery DC. Optimizing stereolithography throughput. J Manuf Syst 1997;16(4):290-303.
24. Davidowitz G, Kotick PG. The use of CAD/CAM in dentistry. Dent Clin N Am 2011;55(3): 559-570.
25. Turkyilmaz I, Wilkins GN, Varvara G. Tooth preparation, digital design and milling process considerations for CAD/CAM crowns: Understanding the transition from analog to digital workflow. J Dent Sci 2021;16(4):1312.
26. Di Francescantonio M, Rocha Pacheco R, Rodrigues Aguiar T, Cidreira Boaro LC, Ruggiero Braga R, Luis Martins A, et al. Evaluation of composition and morphology of filler particles in low-shrinkage and conventional composite resins carried out by means of SEM and EDX. J Clin Dent 2016;13(1):49-58.
27. Palacios T, Abad C, Pradíes G, Pastor JY. Evaluation of resin composites for dental restorations. Procedia Manuf 2019;41:914-921.
28. 3M: Lava™ ultimate CAD/CAM restorative technical product [Internet]; 2015. Available from:https://jensendental.com/wpcontent/uploads/Lava_Ultimate_Technical_Product_Profile.pdf.
29. Yin R, Jang YS, Lee MH, Bae TS. Comparative evaluation of mechanical properties and wear ability of five CAD/CAM dental blocks. MDPI 2019;12(14):2252.
30. Sonmez N, Gultekin P, Turp V, Akgungor G, Sen D, Mijiritsky E. Evaluation of five CAD/CAM materials by microstructural characterization and mechanical tests: a comparative in vitro study. BMC Oral Health 2018;18(1):1-3.
31. Vickers hardness test Wikipedia [Internet]; 2023. Available from: https://en.wikipedia.org/wiki/Vickers_hardness_test.
32. Lawson NC, Bansal R, Burgess JO. Wear, strength, modulus and hardness of CAD/CAM restorative materials. Dent Mater J 2016;32(11): 275-283.